UC Riverside

UC Riverside Electronic Theses and Dissertations

Title

Dissect Epigenetic Regulation in a High-Order Nucleosome Assembly

Permalink

https://escholarship.org/uc/item/1d86b9bg

ISBN

9798180113726

Author

Yoon, Sol

Publication Date

2026-05-29

Peer reviewed|Thesis/dissertation

eScholarship.org Powered by the California Digital Library
University of California

UNIVERSITY OF CALIFORNIA
RIVERSIDE

Dissect Epigenetic Regulation in a High-Order Nucleosome Assembly

A Thesis submitted in partial satisfaction
of the requirements for the degree of

Master of Science

in

Biochemistry and Molecular Biology

by

Sol Yoon

June 2026

Thesis Committee:
Dr. Jikui Song, Chairperson
Dr. Gregor Blaha
Dr. Sihem Cheloufi

Copyright by
Sol Yoon
2026

The Thesis of Sol Yoon is approved:

_____

_____

_____

Committee Chairperson

University of California, Riverside

To my parents and friends, whose constant love, belief in me, and unwavering support have been the foundation of this accomplishment.

ABSTRACT OF THE THESIS

Dissect Epigenetic Regulation in a High-order Nucleosome Assembly

by

Sol Yoon

Master of Science, Graduate Program in Biochemistry and Molecular Biology
University of California, Riverside, June 2026
Dr. Jikui Song, Chairperson

Eukaryotic chromatin is packaged within the nucleus in the form of a highly organized structure, with nucleosomes as basic units. Each nucleosome is comprised of an octamer of histone proteins, wrapped by 147-base pair DNA. The chromatin environment, orchestrated by high-order nucleosome assembly, critically influences various genome activities, such as epigenetic regulation. Increasing evidence has indicated that the multivalent interaction between an epigenetic modifier or effector and the nucleosome array dictates the epigenetic states, and consequently, genome organization and gene activity. To date, due to the complexity of high-order nucleosome assembly, the structure and mechanism of epigenetic complexes have mostly been characterized at the mono- and/or dinucleosome level, which has limited our mechanistic understanding of their nucleosome interactions in a native chromatin environment. To extend this limit, we have reconstituted an epigenetically modified tetranucleosome for protein interaction. In preliminary studies, we measured the nucleosome-binding affinity

of two heterochromatin factors using the electrophoretic mobility shift assay (EMSA). Our long-term goal is to deepen the understanding of how multivalent protein-nucleosome interactions contribute to epigenetic modification and genome organization in cells.

TABLE OF CONTENTS

Introduction 1

Methods 5

Result 10

Discussion 32

Reference 34

LIST OF FIGURES

Figure 1: PCR Condition Optimization..... 10

Figure 2: DNA Sample Quality Test..... 11

Figure 3: Nucleosome Core Particle Reconstitution Condition Optimization..... 12

Figure 4: Negative Stain TEM Image of Free Nucleosome Core Particles..... 13

Figure 5: tetranucleosome-DIM2-HP1 Complex Binding Affinity Test – EMSA..... 14

Figure 6: Negative Stain TEM Image of tetranucleosome-DIM2-HP1 Complex..... 16

Figure 7: EMSA for Grafix..... 17

Figure 8: TEM Image of tetraNCP-DIM2-HP1 Complex on Cryo-EM Grid..... 18

Figure 9: Free tetraNCP Processed cryo-EM Electron Density Map..... 20

Figure 10: Free tetraNCP Processed cryo-EM Electron Density Map – Colored..... 20

Figure 11: Free tetraNCP EMSA after Grafix..... 22

Figure 12: Negative Stain TEM Image of tetraNCP-DIM2-HP1 Complex after Grafix.. 23

Figure 13: DIM2-HP1 Complex Titration of tetraNCP..... 25

Figure 14: DIM2 Mutant-HP1 Complex Titration of tetraNCP..... 28

Introduction

In the nuclei of eukaryotic cells, chromatin is arranged in the form of nucleosome, high-organized structure. Repetitive 147-base-pair-long DNA and a protein histone octamer compose the nucleosome core in the form of DNA wrapping 1.7 left-handed superhelical turns around two octamers: H2A, H2B, H3, and H4 [6][8]. The linker between nucleosome in higher order nucleosomes is 30-base pair long, which make final length of the 601 DNA to be 177-base pair long DNA. The dynamics of chromatin structures present open and closed conformations, where open chromatin exhibit 11nm beads on a string and closed conformation with 30nm fiber [9]. The local arrangement and compaction of chromatin alter DNA accessibility to other nucleosome DNA-interacting factors. DNA of the nucleosome is exposed by nucleosome remodeling proteins by moving histone octamers, instead of fully unwinding DNA from histone octamers. Exposed DNA allows transcription, replication, recombination, and many other processes involving DNA. In addition to physically exposing DNA, epigenetic modification on both DNA and the histone tail is also essential for alterations between open and closed conformation. Especially, Lysine 9 of Histone H3 trimethylation (H3K9me3) and methylation on cytosine of DNA are two of the main instructional mark of nucleosome condensation. DNA methylation induces downstream effect with multiple proteins that triggers further compaction of nucleosomes: for instance, methylated DNA recruits specialized Methyl-CpG Binding Domain (MBD) proteins which further recruits Histone Deacetylases (HDACs). This series of recognizing and binding to epigenetic marks emphasizes how broad the influence of methylated DNA on downstream repressive effect

on chromatin. K9me3 modifications on Histone 3 is also highly correlated with chromatin compaction. H3K9me3 mark is read by the protein HP1 – "reader" for H3K9me3 mark. Recognition and binding of HP1 to H3K9me3, along with oligomerization of HP1 proteins, bridges adjacent nucleosomes together. Clustering nucleosomes causes the chromatin to condense into highly ordered, transcriptionally silent – repressive – form.

In this study, a tetranucleosome is used to escalate understanding of chromatin structure and transformation of its conformation. The tetranucleosome is known as the minimal structural unit of higher-order chromatin folding. It is significantly more stable compared to mono- and dinucleosomes; while tetranucleosome has alternative nucleosomes interact and stack together, mono- and dinucleosomes lack the spatial length to form nucleosome stack, comprising more flexible, unwrapping-prone structure. Due to higher stability of tetranucleosome, it is more adequate to be used for structural analysis of protein-interacted higher-ordered nucleosome. Previously characterized conformations of tetranucleosome – alpha-tetrahedron and beta-rhombus – was used as reference of free tetranucleosome [1][3]. Overall architectures of tetranucleosome are similar regardless of the linker DNA length. Nucleosome 1 and nucleosome 3 form a canonical stack, whereas nucleosome 2 is located in a DNA loop between the two-nucleosome stack. Nucleosome 4 is considered as the outer nucleosome, not being stacked with nucleosome 2. The mobility of nucleosome 2 and 4 increases as nucleosome repeat length (NRL) increases [3]. While multiple proteins can alter the level of nucleosome compaction, heterochromatin factors and DNA methyltransferase are common factor that condense the

nucleosome structure. Defect-In-Methylation-2 (DIM2)-Heterochromatin Factor 1 (HP1) complex is the main nucleosome-interacting protein used to enrich understanding of structural interactions between nucleosomes and them. DIM2 is a DNA methyltransferase in *Neurospora.* What differentiates DIM2 from other DNA methyltransferases for mammalian DNA is that DIM2 can perform *de novo* and maintenance DNA methylation once activated without needs of multiple DNA methyltransferases with different roles overlapping and working together. An increase in region specific DNA methylation activity of DIM2 requires both H3K9me3 and HP1 present. In absence of H3K9me3 and HP1, DIM2 alone might be able to recognize the target DNA but has very little or no methyltransferase activity. Such a characteristic is uniquely found in DIM2, which allows to explore how histone methylation H3K9me3 allosterically guide DNA methylation. One DIM2 molecule requires one HP1 homodimer to form a complex to catalyze DNA methylation efficiently. While DIM2 is responsible for specifically methylating the fifth carbon of the cytosine ring in DNA [8], HP1 is responsible for recognizing the H3K9me3 epigenetic mark by its chromodomain (CD). DIM2-HP1 complex forms by binding of the HP1 homodimer to DIM2 with its chromo shadow domain (CSD). It induces a disorder-to-order transition of the DIM2 N-terminal tail (NT) and target recognition domain (TRD), which is required for methyltransferase activity of DIM2. This is an allosteric regulation of DNA methylation activity of DIM2, via structural stabilization of TRD. DIM2 also interact with histone octamer at K9me3 mark of Histone H3m tail, mediated by both putative replication-foci-targeting sequence (RFTS) and bromo-adjacent homology (BAH1) domains of DIM2. Both H3K9me3-interacting domains play a critical

role in DIM2 interaction with substrate DNA: RFTS-H3K9me3 interaction for locating H3K14 to directly interact with substrate DNA and BAH1-H3K9me3 interaction for rearranging the TRD loop bridging and catalytic core of DIM2 to contact with DNA. Mutations in DIM2 residues that participate in the crucial role of DIM2 lead to drastic hindrance of DNA methylation activity of DIM2 [10]. In order to understand the interaction between nucleosome-binding proteins and tetranucleosome, tetranucleosome and wildtype – unmutated – form of heterochromatin-interacting factors are incubated together for binding affinity tests, negative staining images, and cryogenic electron microscopy (cryo-EM). The cryo-EM structure of the nucleosome and nucleosome-interacting protein together reveals the sites binding of proteins to tetranucleosome. Furthermore, mutated forms of nucleosome-interacting proteins are incubated together to test which domain of DIM2 is involved in DNA-binding activity. Together, this study enhances understanding of the dynamic conformation of the tetranucleosome in the presence of nucleosome-interacting proteins, with the disclosure of structural analysis of their binding.

Methods

4x177 601 DNA purification

Plasmid DNA of 4x177 601 was mixed with stellar competent cells for transformation. The transformed cells were inoculated into 5 mL LB broth with 1 mM Kanamycin antibiotics. The culture tube was shaken overnight, then centrifuged for 15 minutes at 4000 rpm, at room temperature; the supernatant was discarded. The pellet was resuspended with 250 µL of solution I (25 mM Tris-HCl (pH 8.0), 50 mM Glucose, 10 mM EDTA, 100 µg/mL RNase A). 250 µL of Solution II (0.2 M NaOH, 1% SDS) and 350 µL of solution III (3 M Postassium Acetate) has been added, inverted to thoroughly mix. The mixture was centrifuged for 10 minutes to isolate supernatant. Supernatant was applied to the HiBind column, centrifuged down. 500 µL HBC buffer was added and centrifuged down. 700 µL of DNA wash buffer was added to column, centrifuged down. The washing step was repeated three to four times, followed by centrifugation of empty column to dry ethanol from HBC and wash buffer out. Plasmid DNA was eluted out of the column with ddH_2O.

Polymerase Chain Reaction

All final PCR mix volume was 10 mL. 1.5 µg of plasmid DNA, 1 mL 10x PFU buffer, 200 µL of Phusion enzyme, 200 µL of dNTP, 50 µL of forward primer, 50 µL of reverse primer, and ddH_2O were added to the mix. DNA is heated to 95°C for 1 minute, followed by 35 cycles of 95°C denaturation for 30 seconds, 58°C annealing for 30 seconds, and 72°C extension for 25 seconds. The PCR samples stayed at 72°C for 10

minutes for further elongation. PCR was stored in 4°C for short term storage or -80°C for long term storage.

DNA Agarose Gel Extraction

The PCR sample was concentrated into approximately 500 µL from 10 mL. 1.4% of agarose gel with Ethidium Bromide with single wide comb was solidified. 83.3 µL of purple gel loading dye was added to concentrated PCR mix and loaded to gel. Gel-electrophoresis was run until dye reached the bottom. The band of DNA was cut under UV lamp. The cut gel was melted in 14 mL of gel binding buffer in heat plate, and the mixture was cooled down in ice. 700 µL of mixture was added to silica membrane column and centrifuged for 1 minute at 13000 rpm at room temperature. 500 µL of wash buffer was added to column, and repeated for 4 times. Washing step was followed by empty column centrifugation to dry ethanol of wash buffer. 50 µL of ddH_2O was added to elute out DNA from silica membrane column. The concentration of DNA was measured on nanodrop. The integrity of DNA was checked by running 50 ng DNA with loading buffer (10 mM Tris-HCl (pH 8.0), 20% glycerol) in 5% native gel in 0.2X TBE running buffer.

Nucleosome Core Particle Reconstitution

Histone octamer and 5 ng of DNA were mixed in molar ratio of 1:6.5 (DNA:Histone), and centrifuged at 4°C for a few seconds. The sample was transferred into Slide-A-Lyzer MINI Dialysis Units 3,500 MWCO dialysis cup, which was placed in 400 mL high salt KCl buffer (10 mM Tris pH 7.5, 2 M KCl, 1 mM EDTA, 1 mM DTT). The mixture was

gradually dialyzed over 20 hours from high salt buffer to 2 L of low salt buffer (10 mM Tris-HCl (pH 7.5), 0.4 M KCl, 1 mM EDTA, 1 mM DTT). The nucleosome mixture was further dialyzed in HEPES buffer (10 mM HEPES, 50 mM NaCl, 1 mM DTT) overnight. The quality of NCP was checked by running 200 ng of NCP with loading buffer (10 mM Tris-HCl (pH 8.0), 20% glycerol, 100 mM NaCl) in pre-run 4% native gel in 0.2X TBE running buffer.

Electrophoretic Mobility Shift Assay (EMSA) – Nucleosome-protein Binding Affinity Test

Reconstituted nucleosome and DNA binding proteins (DIM2-HP1 complex and AMT complex) were mixed in a molar ratio: 1:1, 1:2, 1:4, 1:8, 1:16. The mixture was incubated in ice for 30 minutes while 4% native gel was pre-running in 0.2X TBE buffer. The nucleosome-protein mixture with loading buffer (10 mM Tris-HCl (pH 8.0), 20% glycerol, 100 mM NaCl) was loaded to gel, ran for 1 hour 30 minutes. Gel was detached from glass plate and stained with SYBR Gold dye, shacking for 10 minutes. The gel was imaged under Bio-Rad ChemiDoc Imaging machine.

Gel Gradient Fixation (GraFix)

200 µg of nucleosome core particles (NCP) in 100-µL volume was prepared by concentrating different NCP samples. In polypropylene tube, top buffer (50 mM HEPES (pH 7.5), 100 mM NaCl, 10% Glycerol) and bottom buffer (50 mM HEPES (pH 7.5), 100 mM NaCl, 30% Glycerol, 0.02% GA) were respectively placed from the bottom of the tube. Cushion buffer (50 mM HEPES (pH 7.5), 100 mM NaCl, 7% Glycerol) was placed at the top of the layer, after removing 200 µL of the top buffer from the top. The sample

was gently placed at the top of the gradient. After balancing the tube holder, the holder was placed into the rotor. The rotor was run for 16 hours at 40,000 rpm at 4°C. After centrifugation, the sample was collected from the top in 500-µL aliquots and placed into individual Eppendorf tubes with 50 µL of 1M Tris (pH 7.5). Samples were subjected to EMSA to check which sample contains the protein bound NCP. The nucleosome-interacting proteins were added to the mixture after GraFix with desired ratio.

Transmission Electron Microscopy [4]

On discharged EM grid, 5 µL of the sample was placed on the carbon side of the grid, allowing the sample to settle on the grid for 1 min. The grid washing step started with applying one droplet of HEPES buffer (20 mM HEPES (pH 7.5), 80 mM NaCl, 1 mM DTT) on the sample side and blot the rinse with blot paper. The washing step was repeated once. 0.5% of Uranyl Acetate stain (negative stain) was applied to the sample side of grid, followed by 1 minute of waiting to allow staining of sample. The excess negative stain was blotted by gently touching the side of grid for 0.5 to 1 second. Using tweezers to hold EM grid, waiting 10 or more minutes for EM grid to completely dry. Negative stain images were acquired under TEM microscope.

Cryo-EM Sample Preparation and Data Collection

After Grafix, the tetranucleosome sample was adjusted to the buffer with 5% Glycerol from 30% Glycerol with 50 mM HEPES (pH 7.5), 100 mM NaCl. Then the post-Grafix tetranucleosome sample was mixed with DIM2/HP1 complex with the ratio of 1:2 (tetranucleosome:DIM2/HP1). Aliquot of 3 µL of tetranucleosome-DIM2-HP1 complex

was loaded to glow-discharged Graphene Oxide (GO) grids or regular grid, based on the consideration of concentration of the sample: high concentration sample was loaded to regular grid while low concentration sample was loaded to GO grid. The grid was blotted for and plunge frozen into liquid nitrogen.

The cryo-EM data was collected on Titan Krios microscope at 300kV at Nation Center for CryoEM Access and Training (NCCAT). The micrographs were acquired in counting mode with energy filter (20eV slit width) at pixel size of ~1.1Å over 40 ms frames, with defocus of -0.6 μm to -2μm.

Results

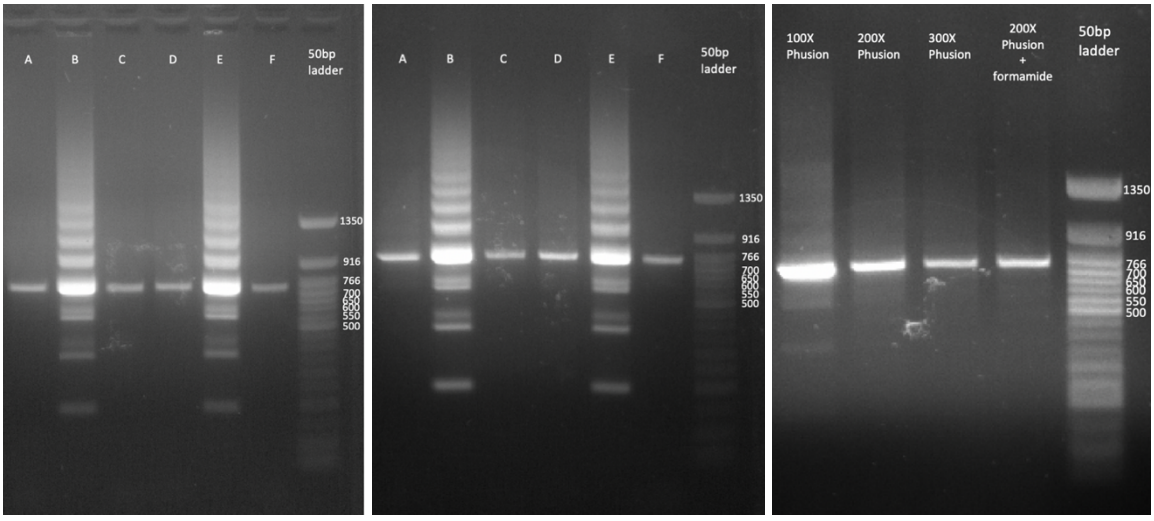


Figure 1: PCR Condition Optimization ((Left) Annealing temperature test – 58°C (A, B, C) and 52°C (D, E, F). Three different DNA polymerase used – A/D: 200x diluted Phusion, B/E: 450x diluted PFU, C/F: HIFI DNA polymerase. (Middle) Extension time test – 25 sec (A, B, C) and 20 sec (D, E, F). Three different DNA polymerase used – A/D: 200x diluted Phusion, B/E: 450x diluted PFU, C/F: HIFI DNA polymerase. (Right) Different concentration of Phusion DNA polymerase test – different dilution of Phusion polymerases were tested. Only difference in PCR mixture is dilution of Phusion)

Multiple polymerase chain reactions (PCR) were performed to determine which condition yielded the fewest impurities and the greatest amount of PCR product (Fig. 1). Since the size of the 4x177 601 DNA was around 726-base pairs, the target band size was determined using the 50-base-pair marker. First, different PCR programs were tested in order to determine the optimal annealing temperature for different DNA polymerases. Everything else but the annealing temperature was constant throughout different conditions. Between 58°C and 52°C, while there was no recognizable difference in impurities in terms of Phusion and HIFI DNA polymerase, the 58°C program resulted in a slightly brighter band: the brighter the band, the more PCR product obtained; the final annealing temperature was fixed to 58°C. The quality of PCR product using different DNA polymerases was also tested: Phusion DNA polymerase, PFU DNA polymerase,

and HIFI DNA polymerase. Each DNA polymerase dilution was made with their dilution buffers — for instance, Phusion dilution buffer for Phusion DNA polymerase. Among different DNA polymerases, Phusion and HIFI resulted in the least impurities, while PFU DNA polymerase still had multiple bands, indicating the presence of impurities. Lastly, to test the influence of DNA polymerase concentration on the impurities, multiple dilution of Phusion DNA polymerase were used for the PCR test. 100 times diluted Phusion DNA polymerase (from undiluted 1.5mg/mL Phusion) resulted in the brightest band, while the impurities were relatively similar throughout the dilutions.

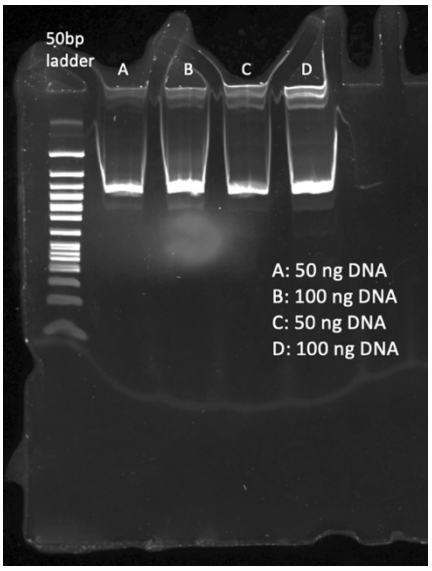


Figure 2: DNA Sample Quality Test (4x177 601 DNA was loaded to 5% native gel for EMSA to check the quality of the DNA.)

Before obtaining the tetranucleosome using purified DNA, a quality check for DNA sample was done in order to reduce the possibility of impurities due to contamination (Fig. 2). The sole purpose of the quality check was to determine if there is any significant contamination within the DNA sample that can cause an impure tetranucleosome sample after the reconstitution. A few bands present at the top of the gel

are impurities within the sample; however, that was not significant enough to dominate the component of the purified sample. An increase in the concentration of the total DNA sample loaded resulted in brighter impurity bands, although the relative brightness of those bands was dimmer than the target band around 700-base-pair marker. The quality check of DNA sample stated that the DNA sample was pure enough to be used for tetranucleosome reconstitution.

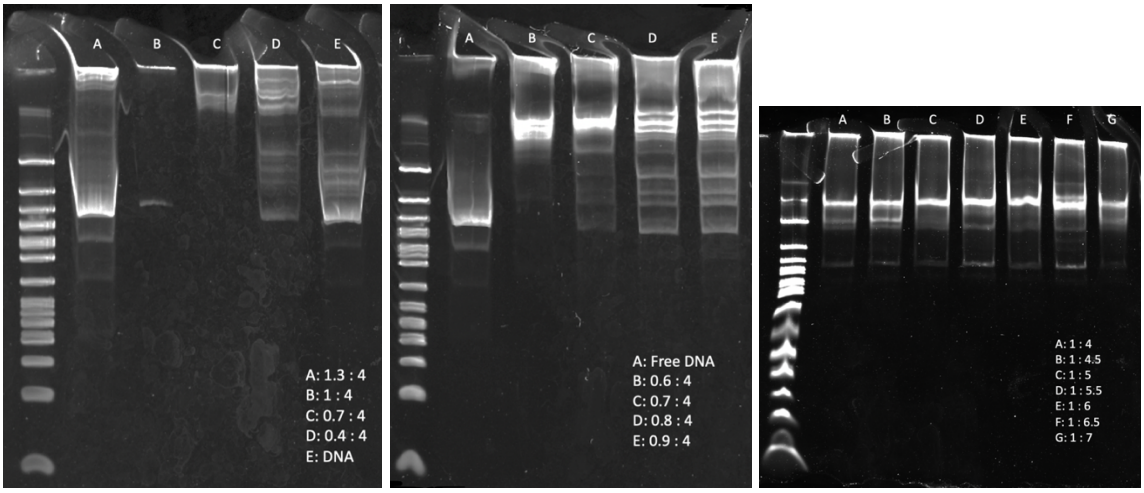


Figure 3: Nucleosome Core Particle Reconstitution Condition Optimization (4x177 601 DNA to histone octamer is labeled on image. Free DNA (sample A) followed by nucleosome with different ratio of DNA to histone octamer are loaded to 4% native gel for EMSA)

After purifying DNA, different ratios of 4x177 601 DNA to histone octamer were tested to determine the optimal ratio for tetranucleosome production (Fig. 3). 4% native gel for EMSA was used to improve the distance of band traveling due to the large size of the tetranucleosome. The size, brightness, and number of bands for each ratio were the main reference for nucleosome reconstitution conditions. The target tetranucleosome band was around 1350-base pair large. Among the ratio, 1:5 to 1:6 resulted in a bright singular band. Leftover DNA after reconstitution was present regardless of the ratio; therefore, the focus of determining the ratio was the brightness of the singular band and

number of bands present in sample. For every new DNA sample purified, the ratio optimizations were done in order to define the best ratio used to reconstitute the tetranucleosome. The optimal ratio of DNA to histone octamer varied for each purified DNA, although they tended to fall within the range of 1:5 to 1:6.

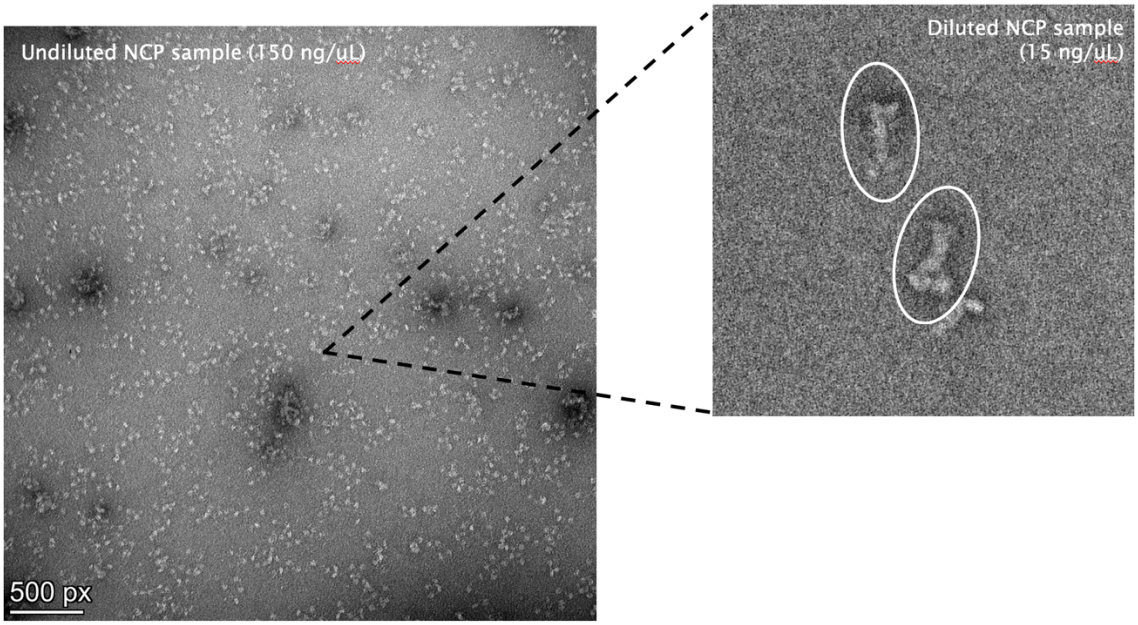


Figure 4: Negative Stain TEM Image of Free Nucleosome Core Particles ((Left) Undiluted sample (concentration of 150 ng/µL) of tetranucleosome image taken under Negative Stain Transmission Electron Microscopy. (Right) 10 times diluted sample (15 ng/µL) of tetranucleosome image taken under Negative Stain TEM. Identical method and condition for TEM was used for both samples)

Negative stain TEM images of the reconstituted tetranucleosome without any nucleosome-interacting factors were obtained in order to determine the homogeneity of the sample (Fig. 4). The image of the undiluted sample contained relatively homogeneous particles throughout the grid, although it was not highly populated. The low particle density was due to a moderate concentration of the sample, as the number of particles increased with increasing concentration. The dark spot in the image was due to the accumulation or crystallization of the Uranyl Acetate stain – a stain used for contrast and

fine-grain resolution of negative TEM images – causing spatial precipitation and aggregation of the loaded tetranucleosome sample [5]. The precipitation on the grid does not indicate actual precipitation of the sample. The diluted sample provided a more detailed view of individual tetranucleosomes. As previous papers have identified, the two tetranucleosomes found in the negative stain image of the diluted sample have an intermediate structure of alpha-tetrahedron and beta-rhombus; two nucleosome heads are on each side of the linker. Such a result indicated that the structure of the reconstituted tetranucleosome presented as expected.

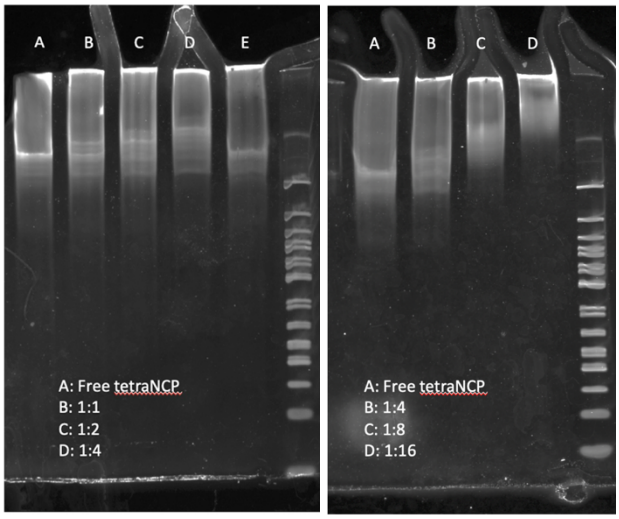


Figure 5: tetranucleosome-DIM2-HP1 Complex Binding Affinity Test - EMSA (Binding affinity test of tetranucleosome with DIM2-HP1 with labeled ratio. 200ng of tetranucleosome with corresponding amount of DIM2-HP1 complex (5uM) were loaded.)

Binding affinity tests of tetranucleosome and DIM2-HP1 complex with different ratios were performed to test the binding intensity of the DIM2-HP1 complex to Tetranucleosome (Fig. 5). DIM2-HP1 complex generally bound to the linker DNA of the multi-nucleosome complex through the cleft between the catalytic core and TRD of DIM2 [10]; three DIM2-HP1 complexes were expected to bind to one tetranucleosome on

their linkers. The overall gradual upward shifts of the band indicated the binding of DIM2-HP1 complex to the tetranucleosome. The size of the DIM2-HP1-bound tetranucleosome increased as more DIM2-HP1 complex interacted with the tetranucleosome, represented by the increase in number of bands with larger size based on the size marker. While the free tetranucleosome (tetraNCP) presented a single band, addition of DIM2-HP1 complex caused the band to not only shift upward but also increase in number of bands and eventually blur out. Additionally, any impurities presented on the tetranucleosome sample could be free DNA or incomplete tetranucleosome, which also interact with the DIM2-HP1 complex. This resulted in disappearing of any bands of impurities as the protein complex ratio increased. This indicated that the DIM2-HP1 complex tend to bind to tetranucleosome even if the tetranucleosome structure was incomplete, as long as the essential material – linker DNA – was present. Such a pattern of DIM2-HP1 complex interaction was also shown in the mixture where free 4x177 601 DNA was present, with the disappearance of the free DNA band as the concentration of the DIM2-HP1 complex increased. Once the tetranucleosome was saturated with DIM2-HP1 complex, there was no longer a free tetranucleosome band present on the gel. A ratio of 1:8 was enough DIM2-HP1 complex amount to make the free tetranucleosome band disappear. Further results of negative stain images of the tetranucleosome-DIM2-HP1 complex led to the conclusion that if the tetranucleosome was highly saturated with DIM2-HP1 protein complex, it may cause a darker spot with a clump of tetranucleosome within the sample. Same pattern was shown

with further increase in concentration; the multivalent characteristics of DIM2 would be the reason for the tetranucleosome clusters [10].

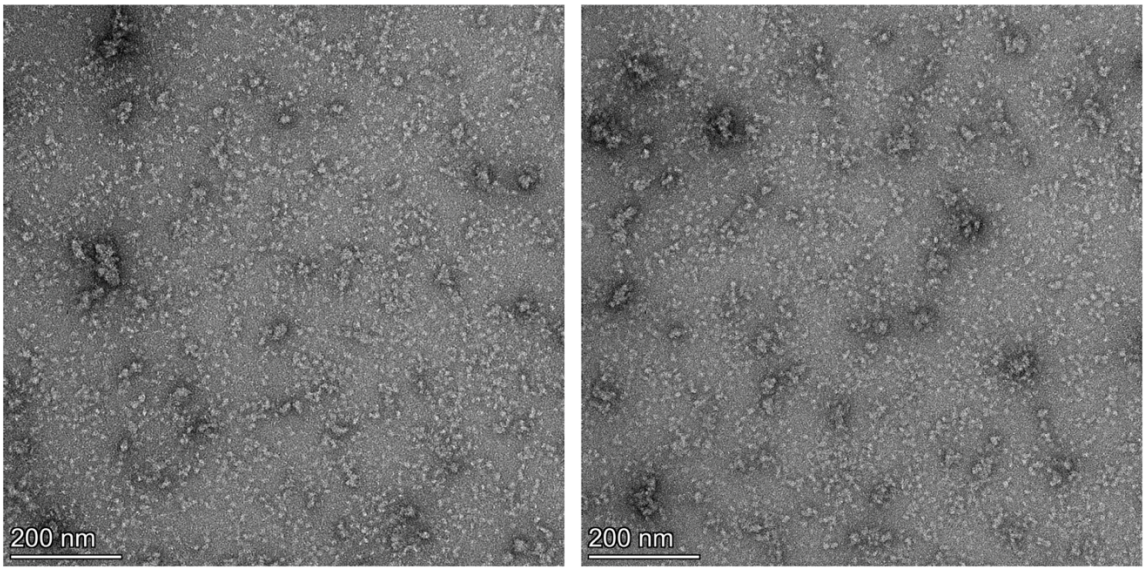


Figure 6: Negative Stain TEM Image of tetranucleosome-DIM2-HP1 Complex (tetranucleosome-DIM2-HP1 complex mixed with the ratio of tetranucleosome to DIM2-HP1 as 1:8)

The mixture of tetranucleosome and DIM2-HP1 complex image was obtained under negative stain TEM (Fig. 6). The ratio of the mixture was 1:8 (tetranucleosome: DIM2/HP1). Due to the low concentration of the tetranucleosome after reconstitution, the sample loaded was undiluted, resulting in a highly crowded particle image. The size differences between tetranucleosome and DIM2-HP1 complex were not as significant under negative stain images as they could not be differentiated: the magnitude of the image was adjusted to view the tetranucleosome mainly, so it was harder to visualize smaller protein complex particles. A few dark spots also appeared in these images, either due to Uranyl Acetate stain used for negative TEM or having tetranucleosome fully saturated by DIM2/HP1 complex, causing multimerization of DNA methyltransferase [5]. The multimerization of DNA methyltransferase – DIM2-HP1 complex – could form

linear oligomer or bridges between multiple nucleosomes; this eventuated in the clusters of tetranucleosomes with a darker background. Hence, though it was not able to differentiate DIM2-HP1 complex from tetranucleosomes, the presence of DIM2/HP1 was indicated from the aggregation-like tetranucleosome constellation in the negative stain images of a saturated tetranucleosome sample.

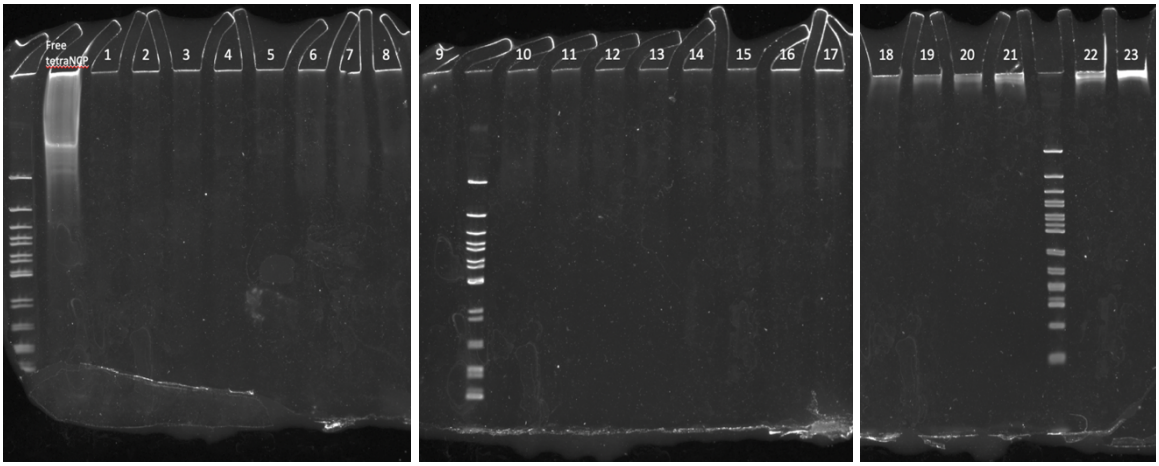


Figure 7: EMSA for Grafix (20μL of each sample collected from Grafix were loaded to 4% native gel. Sample 23 was collected for further process for cryo-EM)

After the tetranucleosome samples were concentrated to a total of 200μg, sample was mixed with the DIM2-HP1 complex, undergoing the GraFix process. Due to the fact that tetranucleosome was highly saturated with the complex – mixed at a 1:8 ratio, the target band tended to appear at the bottom of the Grafix tube (Fig. 7). This meant that binding of the DIM2-HP1 complex made the size of the final protein-bound tetranucleosome large, since larger complex tend to be placed at the bottom of the tube. The large size of the complex caused sample to be not able to fully travel down the gel, even if the gel was a 4% native gel. Based on the gel image, the tube contained the complex was the tube 23. The sample was not able to fully travel down the gel, which made it unable to check the possible impurities contained in the sample. The possibility

of impurities in sample was caused by additional process after the GraFix, such as reducing the glycerol concentration or concentrating the sample for long amount of time.

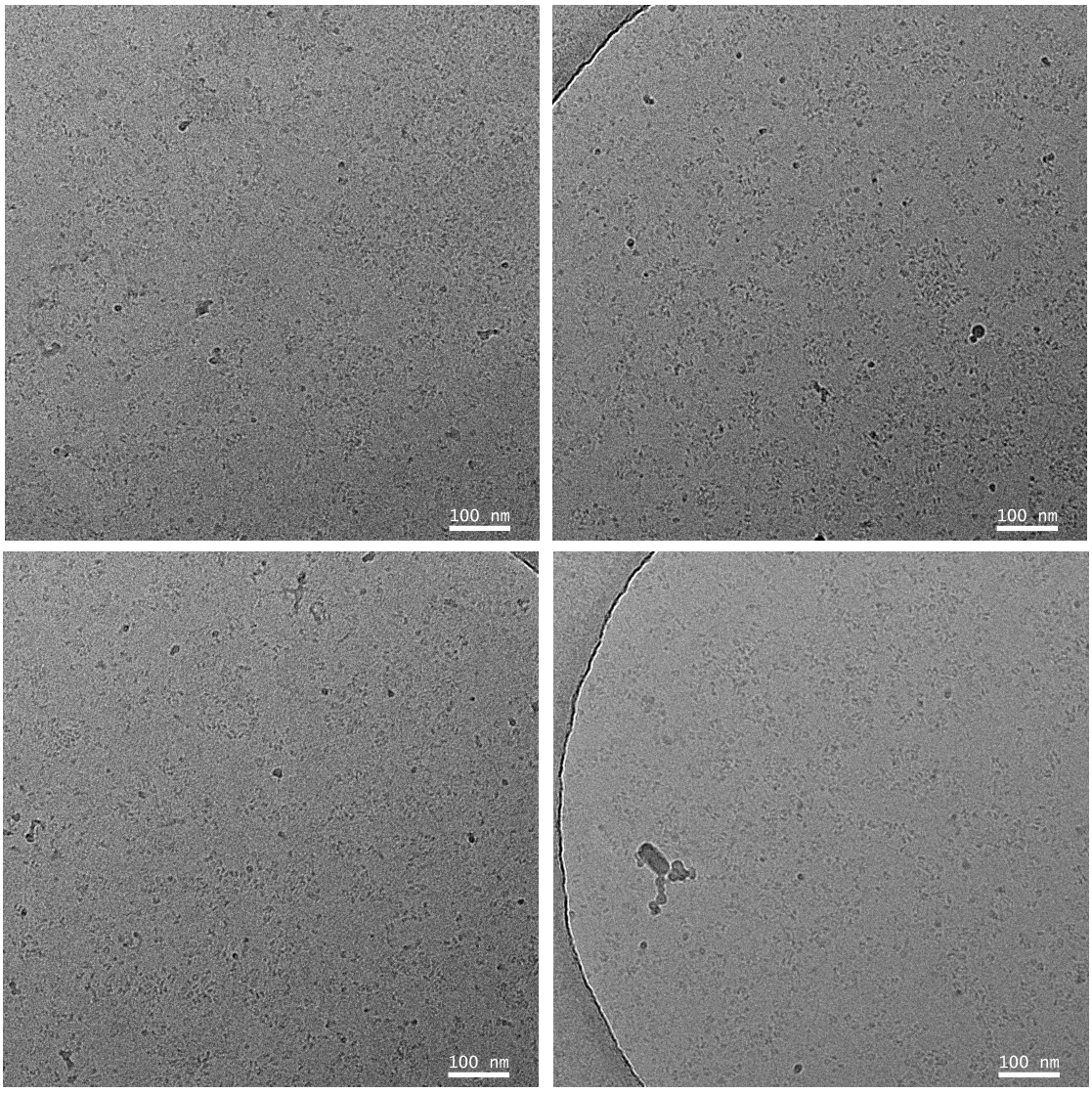


Figure 8: TEM Image of tetraNCP-DIM2-HP1 Complex on Cryo-EM Grid (tetraNCP-DIM2-HP1 complex after decreasing to 5% glycerol from 30% glycerol then concentrated to 100µL. Grid for negative TEM used was GO grid for Cryo-EM)

The concentrated sample, after reducing the glycerol component within the sample, had a low concentration; hence, a Graphene Oxide (GO) grid was used due to multiple reasons (Fig. 8). GO grids have high physical attraction and binding of the

tetranucleosome-DIM2-HP1 complex to the GO surface and have air-water interface protection: if not protected, proteins often show aggressive denaturation or stick to the air-water interface [7]. Such a low concentration of the sample might have been due to multiple processes after GraFix. While sample tube 23 was collected, the process of decreasing glycerol concentration from 30% to 5% glycerol by adding buffer excluding glycerol (50mM HEPES (pH 7.5), 100mM NaCl, 5mM DTT) caused the aggregation of tetranucleosome and proteins together. Glycerol is an essential stabilizing osmolyte that maintains a "hydration shell" around the protein surface. It protects the histone octamer in native, compact conformation by preventing interaction of hydrophobic patches with each other. Such exposure of the hydrophobic regions of the histone octamer protein can cause unfolding of the histone core or exposing of aggregation-prone hydrophobic surface [2]. The thermodynamic equilibrium of the positively-charged histone tails had been shifted – no longer naturally repelling each other – could also allow tetranucleosomes to agglomerate. Furthermore, the multivalence of DIM2-HP1 protein, which led the protein to interact with multiple nucleosome and themselves at once, produced aggregation-like formation where multiple tetranucleosomes are bound together as a big cluster. Compared to the tetranucleosome amount, a large amount of DIM2-HP1 complex was added, causing single proteins to bind to multiple tetranucleosomes simultaneously, cross-linking – bridging – them together. Due to the low concentration of the sample, there was only a few aggregations on the negative stain images. Even though there were distinguishable amount of particles present, the cryo-EM structure obtained was unexpected (Fig. 9). There was no density of the DIM2-HP1 present in the cryo-EM

data, indicating that those tetranucleosomes that were bound to DIM2/HP1 might have been all precipitated out in the process of glycerol adjustment and concentration.

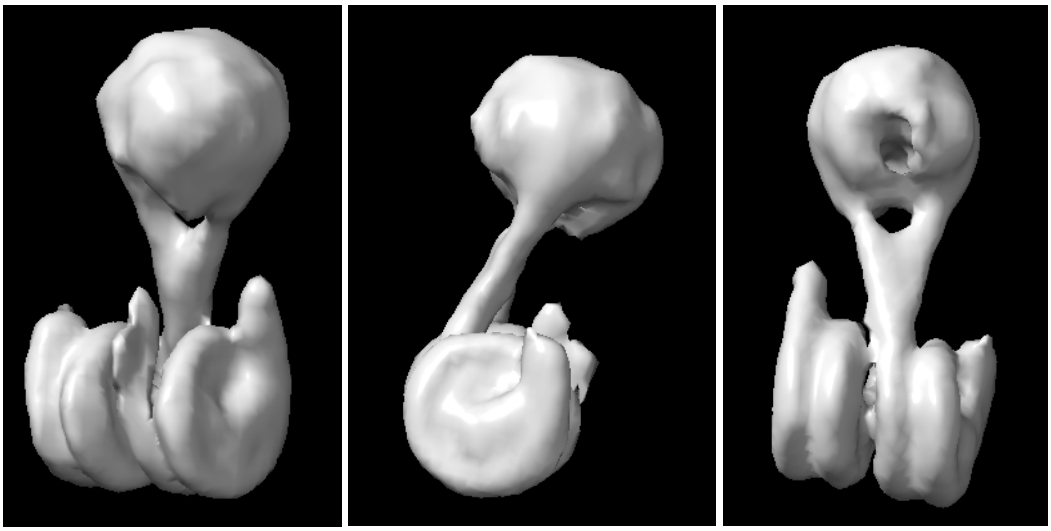


Figure 9: Free tetraNCP Processed cryo-EM Electron Density Map (After data collection, the micrographs were collected then processed. Electron density map was adjusted to only present tetraNCP by removing electron density around the structure.)

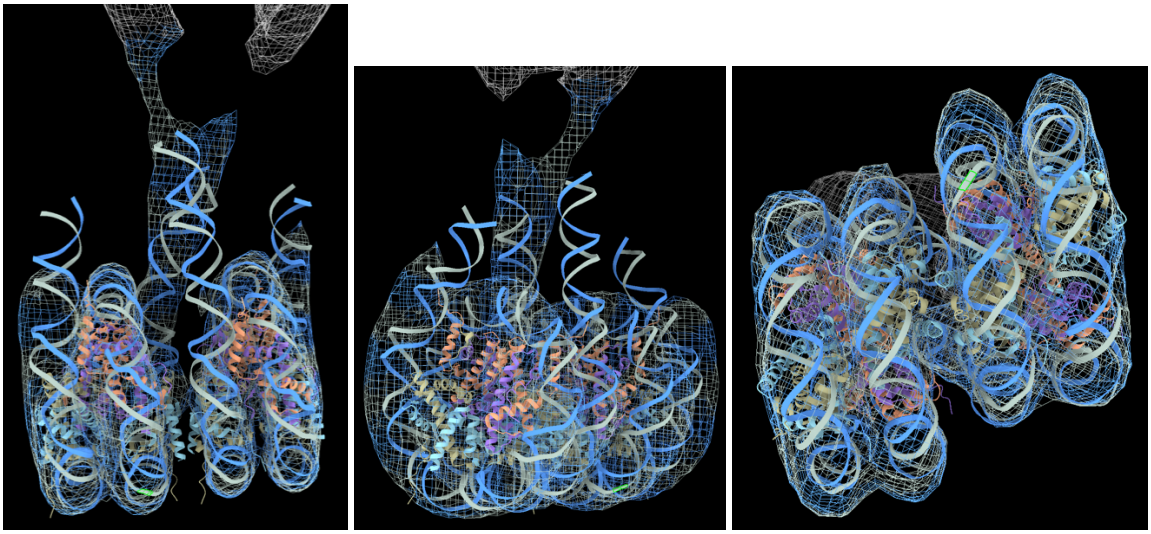


Figure 10: Free tetraNCP Processed cryo-EM Electron Density Map – Colored (The structure of nucleosome canonical stack from PDB was overlapped with free tetranucleosome electron density map. Mesh line is the outer line of the tetranucleosome while DNA (177-base pair long) and histone octamer structure file were saved from PDB.)

Due to the precipitation of DIM2-HP1-bound tetranucleosomes, the resulting cryo-EM data only showed free tetranucleosomes (Fig. 9). Nucleosome 1 and

nucleosome 3 were placed next to each other, which was considered as a canonical stack. Nucleosome 2 was located between the stack, but nucleosome 4 was quite indistinguishable; due to the fluctuation of the nucleosome 4, it was unable to define clear electron density of nucleosome 4 from the collected cryo-EM data. Even though nucleosome 2 was present in the electron density map, the structure of nucleosome 2 was not similar to the nucleosome 1 and 3; this blub-like structure could also be due to the fluctuation of the nucleosome 2 density in the data. Nucleosome 2 is located in between the nucleosome stack; hence it was less dynamic than nucleosome 4, easier to identify the presence of the nucleosome. On the other hand, nucleosome 4 is the outer one and harder to establish its structure due to higher structural heterogeneity. The structure of nucleosome 1 and 3 were clearly presented, with the small tail of the histone core. Once the electron density data of free tetranucleosome canonical stack was obtained, it was overlapped with previously defined structure of the stack (Fig. 10). Some portions of the structure that were not fully overlapped due to missing linker DNA of obtained electron density. Other than small DNA fragments, the DNA wrapped histone octamer structure of the canonical stack were well matched with known structure of the stack. Furthermore, even with the low resolution of the structure, it was able to determine the major and minor groove. Although the sample was mixed with the DIM2-HP1 complex, the electron density of DIM2-HP1 was not observed due to loss of DIM2-HP1-bound tetranucleosome. It was unable to anticipate that only cryo-EM structure of free tetranucleosome would be obtained from the negative stain TEM image, since it was difficult to differentiate DIM2-HP1-bound tetranucleosome from free ones. Thus, with

missing DIM2-HP1 from the final cryo-EM results and having only free tetranucleosome on the collected data, it was possible to conclude that adding the concentration of DIM2-HP1 complex that were enough to saturate tetranucleosome had caused precipitation of complex-bound tetranucleosomes. In order to improve the loss of DIM2-HP1-bound tetranucleosome for cryo-EM, the process of stabilizing tetranucleosomes was adjusted to minimize possible precipitation.

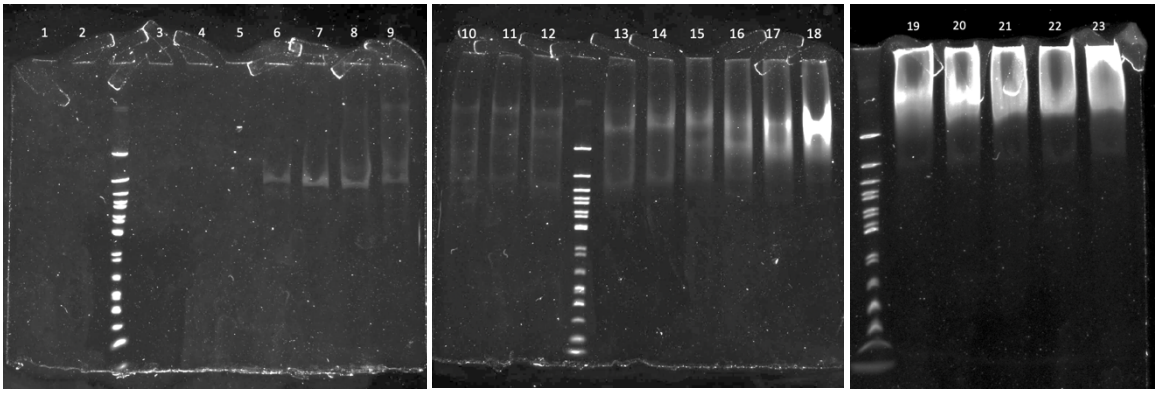


Figure 11: Free tetraNCP EMSA after Grafix (20µL of each free tetranucleosome sample collected from Grafix were loaded to 4% native gel. Sample 19, 20, 21, 22, 23 were collected and concentrated after the glycerol concentration was reduced to 5% from 30%)

Since the loss of target complex happened during glycerol adjustment and concentration after Grafix, mixing of tetranucleosome and DIM2-HP1 complex was done after the GraFix of free tetranucleosome. Grafix process stabilized the fragile, flexible tetranucleosome by providing intramolecular cross-linking – exposing nucleosomes to a chemical fixative, locking the highly dynamic tetranucleosome into a compact, folded conformation with the fixative, and preventing dissociation to inhibit unfolding of the complex – by chemically "freezing" the interaction [2][11]. Due to the stabilization, reducing glycerol percentage and concentration of multiple tetranucleosome samples (tube 19, 20, 21, 22, and 23) would not produce precipitation of tetranucleosome (Fig.

11). After the concentrating step, the sample was tested in order to check the quality. There were some DNA fell out of the tetranucleosome after concentration, which might be due to lowering the glycerol percentage from 30% to 5%; however, the brightness of the tetranucleosome was much higher than the free DNA band, making it possible to use for further experiment without interference from free DNA. Even if there were some free DNA that interacted with DIM2-HP1 complex, those cryo-EM data would be discarded during the date process.

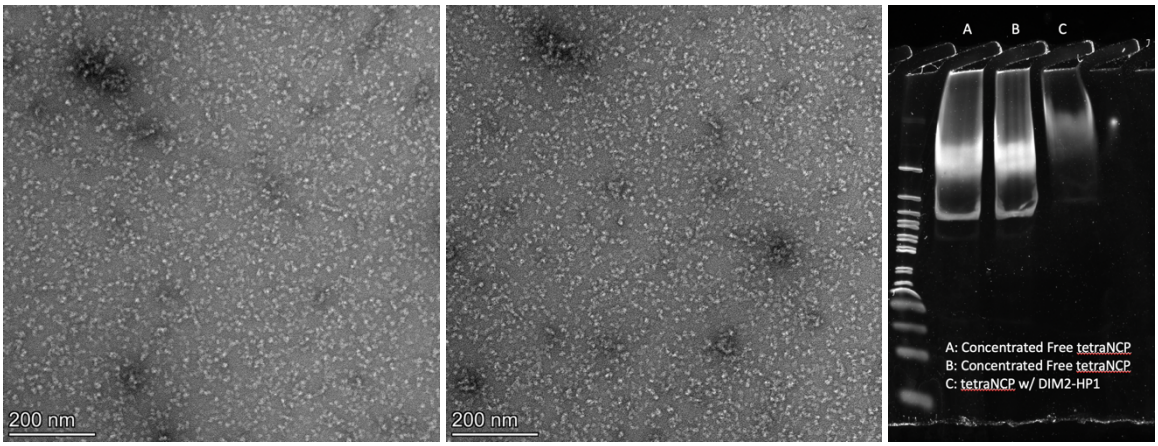


Figure 12: Negative Stain TEM Image of tetraNCP-DIM2-HP1 Complex after Grafix ((Left/Middle) tetraNCP after Grafix, decreasing to 5% glycerol from 30% glycerol then concentrated to 100µL, and DIM2-HP1 complex added. (Right) 4% Native Gel Image of free concentrated tetraNCP and after tetraNCP mixed with DIM2-HP1 complex.)

After the Grafix, the tetranucleosome sample was mixed with the DIM2-HP1 complex for better binding of the nucleosome-interacting protein with the nucleosome. The possibility of complex precipitation was relatively lower than in the sample that had a DIM2-HP1-tetranucleosome mix before GraFix. The sample had a higher concentration and was homogeneous enough to consider that the tetranucleosomes were not precipitated out, given that more sample tubes were collected to be combined together (Fig. 12). The ratio used for DIM2/HP1 complex amount was 1:2 (tetranucleosome to

DIM2-HP1 complex). The ratio was lowered since a high concentration of DIM2-HP1 complex acted as multivalent proteins, causing aggregation of multiple tetranucleosomes. It made the sample unable to obtain its structure through cryo-EM. Even though less amount of DIM2-HP1 complex was added, the complex still had sufficient binding to tetranucleosome; on the 4% gel image, the band was shifted upward compared to the free tetranucleosome, indicating the presence of binding of DIM2-HP1 complex to tetranucleosome. Due to 1:2 ratio of mixture, tetranucleosomes were not completely saturated; thus, there was no significant aggregation under negative stain images except those due to the UA stain [5]. The concentration of the sample was around 180 ng/μL, which was high enough to use a regular cryo-EM grid. Negative stain TEM images of the DIM2-HP1-bound tetranucleosome particles were taken immediately after mixing, followed by preparation of the cryo-EM grid with a regular grid.

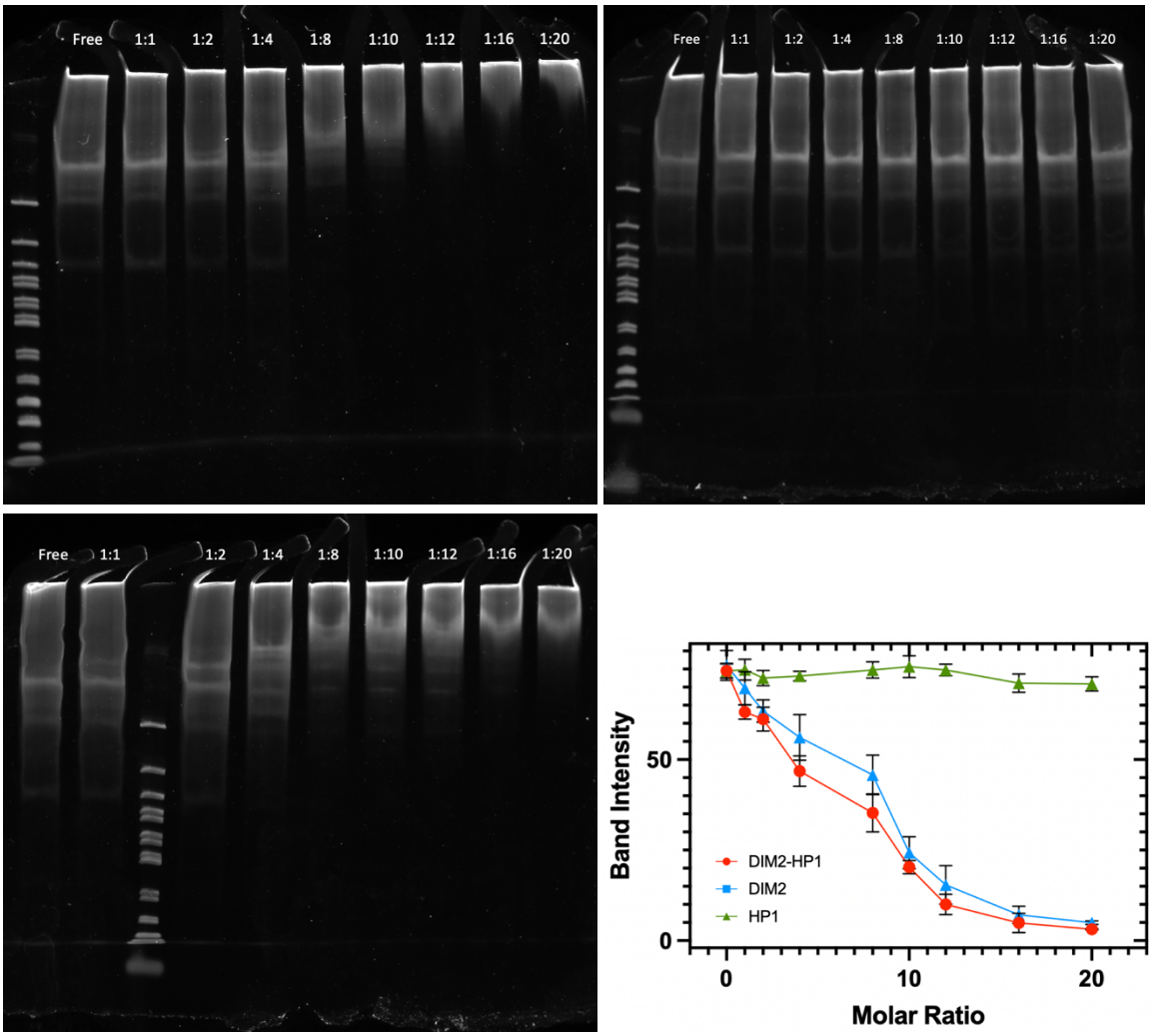


Figure 13: DIM2-HP1 Complex Titration of tetraNCP ((Top Left) EMSA for different ratio of DIM2 added to tetraNCP. (Top Right) EMSA for different ratio of HP1 added to tetraNCP. (Bottom Left) EMSA for different ratio of DIM2/HP1 complex added to tetraNCP. (Bottom Right) Band Intensity vs. Molar Ratio graph for wildtype DIM2.)

To compare the level of binding of DIM2 and HP1 individually to the DIM2-HP1 complex, the binding affinity was tested with an increasing ratio of tetranucleosome to DIM2-HP1 complex first, until the tetranucleosome became fully saturated (Fig. 13). An increase in the concentration of DIM2-HP1 complex bound to tetranucleosome resulted in increasing the size of the overall complex. As the number of tetranucleosomes bound to the DIM2-HP1 complex increased, the band for the final complex shifted more

upwards. However, the upward shifting of the band did not continue infinitely. Starting around the ratio 1:12, the bands were located at the same level regardless of further increase in the DIM2-HP1 concentration. No notable difference in band size indicated that the tetranucleosome had been fully saturated; thus, there was no DNA site available on the complex to further bind to. Increasing the concentration of protein complex would not be shown in the gel since the dye only stained DNA, not proteins. No matter how much of the free protein complexes were present, the DNA size would be same as fully saturated one with no indication of leftover protein complex. With the same ratios used for tetranucleosome to DIM2-HP1, the binding affinity test for individual DIM2 and HP1 was also performed and checked on 4% native gel. When more DIM2 was added to the tetranucleosome, more binding of DIM2 to the tetranucleosome took place. The gradual upward shift and reduce in intensity of the free tetranucleosome band indicated that there was more binding of DIM2 to the tetranucleosome, increasing the overall size of the complex. From the gel image, the bands of the last three ratios were unable to differentiate from the background. This may be due to the gel quality or intensity of the band since the lines seemed to be smeared. However, through comparing only DIM2 activity to DIM2-HP1 complex between a 1:1 ratio and 1:8 ratio, DIM2-HP1 complex at 1:4 had a higher shift than that of DIM2 alone, as well as 1:8. This higher shift defined that the binding of DIM2-HP1 had slightly stronger binding to tetranucleosome compared to DIM2 itself. The presence of a homodimer of HP1 helped direct DIM2 to the correct chromatin locations in addition to significantly enhancing their catalytic activity. While HP1 was absent in the complex, DIM2 was still able to recognize DNA strands and bind

to them. The influence of HP1 on DIM2 binding to tetranucleosome was not dominant; thus, DIM2 alone still displayed efficient binding to tetranucleosome. On the other hand, free HP1 did not show any interaction with tetranucleosome, which was portrayed as no shift or the decrease in the intensity of the tetranucleosome bands on EMSA. The size of the HP1 protein is roughly 25kDa, relatively smaller than DIM2 proteins. Consequently, binding of HP1 to H3K9me3 histone tails of tetranucleosome did not significantly change the size of the complex: no upward shift resulted on the gel image. Furthermore, HP1 tended to have weaker binding to tetranucleosome, unless divalent binding of HP1 and cross-linking between each other present. The binding of HP1 alone has significantly weak affinity compared to DIM2 and the DIM2/HP1 complex. The intensity of the binding to tetranucleosome decreased in order of DIM2/HP1, DIM2, and HP1. The band intensity vs. molar ratio graph also showed the identical pattern of binding affinity to the gel image. The band intensity of the free tetranucleosome was measured for every molar ratio, while the standard deviation of the band intensity was obtained by replicating the binding affinity test. The band intensity of the free tetranucleosome decreases as more nucleosome-interacting proteins were added. Although, compared to HP1, DIM2 had higher binding affinity to tetranucleosome, it still had weaker binding than the DIM2-HP1 complex.

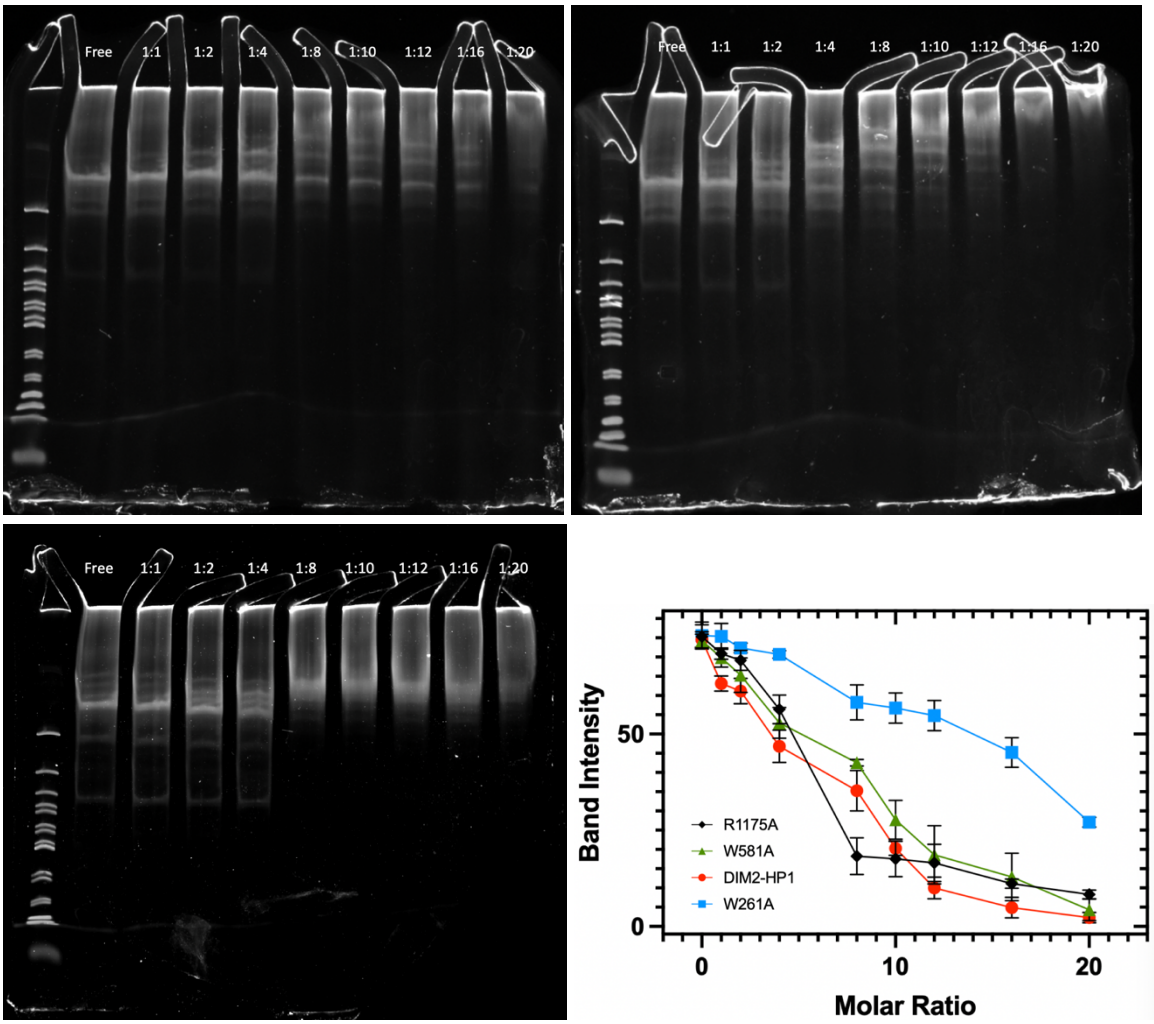


Figure 14: DIM2 Mutant/HP1 Complex Titration of tetraNCP ((Top Left) EMSA for different ratio of W261A DIM2 added to tetraNCP. (Top Right) EMSA for different ratio of W581A added to tetraNCP. (Bottom Left) EMSA for different ratio of R1175A complex added to tetraNCP. (Bottom Right) Band Intensity vs. Molar Ratio graph for mutant DIM2)

The binding affinity tests of the DIM2 mutants in complex with HP1 were also performed in order to determine which domain of DIM2 is crucial for binding to a tetranucleosome (Fig. 14). W261A mutant of DIM2 has a mutation in the RFTS – replication-foci-targeting-sequence – domain, which works cooperatively with the BAH1 domain to recognize and read histone H3K9me3 marks. It forms an active, supplementary DNA-binding site that facilitates substrate association [10]. The mutation in the RFTS

domain could lead to an impaired ability to bind DNA and recognize H3K9me3 histone modification, resulting in significantly lower affinity for DNA. There was still some level of binding of the W261A mutant to tetranucleosome, which was indicated by the increase in the number of larger size band and decrease in the intensity of the tetranucleosome band. This result indicated that there was some binding of the W261A mutant DIM2-HP1 to tetranucleosome, which could be due to presence of regular BAH1 domain and HP1. However, the binding was not strong enough for the complex to fully saturate the tetranucleosome. Hence, having the W216A mutation on the RFTS domain of DIM2 resulted in a lower binding affinity for DNA than wildtype DIM2 due to a decrease in the ability of actual DNA binding as well as recognizing histone marks. The second mutation on DIM2 tested was W581A mutant. Such a mutation was on the W581 of BAH1 – bromo-adjacent homology – domain of DIM2. BAH1 domain displays a role as an epigenetic sensor and allosteric switch. It works with the RFTS domain to recognize and bind to the H3K9me3 histone mark [10]. The mutation on BAH1 disrupts its catalytic activity by maintaining DIM2 in its inhibited state. Loss of the ability to read histone modification disables the conformational switch for activating the DNA-methylating conformation of DIM2. Even so, the DNA-binding activity of the W581A mutated DIM2-HP1 complex was similar to the wild-type DIM2-HP1 complex. Such a result was due to the presence of HP1 and regular RFTS domain. DIM2 relies on multi-layered, redundant activation mechanism; Triggering a disorder-to-order structural transition, which is required for DIM2 binding to DNA, can happen even when BAH1 is mutated with presence of HP1, primarily interacting with TRD of DIM2. Even though the

mutation caused DIM2 itself to decrease in its recognition activity, DIM2's ability to bind to DNA is still heavily dependent on HP1 and other domains in terms of allosteric structure ordering of TRD – target recognition domain. Hence, a mutation could be compensated by the presence of HP1 and RFTS domain, not only by restoring the ability to recognize histone modification but also by stimulating the TRD domain to recognize and bind to the DNA substrate. Lastly, the DIM2 mutant with the mutation of R1175A on TRD – target recognition domain – was tested for binding affinity. It disrupted the activity of TRD, which is critical to DNA substrate binding of DIM2 [10]. The single point mutation in the TRD domain may have caused loss of some binding activity of DIM2, but the presence of HP1 also compensated for such loss to some level. Since DIM2 is a multivalent protein, even after a single arginine mutation disrupted the TRD interface, the N-terminal tail maintain to be intact and continue to interact with HP1. This interaction induced activation and stabilization of DIM2, creating the cleft for DNA to be bound. Due to those factors, a single point mutation might weaken the affinity but did not fully interrupt the role of TRD in DIM2. Such features were demonstrated in the titration. There was no significant binding of the mutant DIM2/HP1 until a 1:2 ratio, while between a 1:4 and 1:8 ratio there was a notable upward shift of the bands. Compared to the wildtype, the change in distance of bands traveled from 1:4 to 1:8 mutant was similar to the change from 1:2 to 1:4 of wildtype. However, the binding of R1175 DIM2-HP1 mutant with higher concentration showed drastic increase in binding to tetranucleosome. This result could be done because of the mass action, where the concentration allowed weaker, non-canonical interactions to take hold despite the mutation. Furthermore, the

presence of regular RFTS domain and BAH1 domain still could associate with DNA, due to the multivalent network of DIM2 domains. The result defined that the R1775A mutant still displayed binding activity to tetranucleosome, although the wildtype DIM2-HP1 still had slightly stronger binding to tetranucleosome than the mutant with higher concentration of complex. Therefore, the domain that influences binding ability of DIM2 the most would be RFTS domain, followed by BAH1 and TRD domain. While the binding of DIM2-HP1 complex to tetranucleosome significantly abolished when mutation was present in RFTS domain, BAH1 mutant and TRD mutant showed similar or slightly weaker binding activity compared to the wildtype. Thus, depending on the domain of DIM2, a single point mutation can lead to various levels of influence on binding activity of DIM2 – from complete loss of activity to similar but weaker activity compared to wildtype DIM2.

Discussion

The interaction of higher-order nucleosomes with nucleosome-interacting proteins deepens the understanding of how different factors influence the nature of nucleosome structure. Heterochromatin and euchromatin are present as fundamental units of DNA storage and processing within eukaryotic cells. Optimization of in vitro reconstitution of tetranucleosome enables further experiments regarding higher-order nucleosome interaction with other proteins. This field of study has not been fully understood compared to lower-order nucleosomes due to the unstable nature of the tetranucleosome, being prone to unfolding or aggregation. During optimization of the tetranucleosome, its instability tended to be present more in large-scale reconstitution: multiple small-scale reconstitutions resulted in a more stable tetranucleosome. Tetranucleosome also tended to be more stable with high glycerol concentration; the GraFix process was necessary in order to increase its stability. In addition to production, multiple proteins were incubated with the tetranucleosome to test their activity on the nucleosome. Epigenetic regulation – transcriptional repressor – was the main goal of the research because higher-order oligonucleosome directly related to an increase in compaction of chromatin, leading to repression of DNA processing. The main protein was DIM2, which has DNA methyltransferase activity with presence of HP1. DIM2-HP1 complex interacts effectively with the oligonucleosome. It primarily acts to methylate DNA within heterochromatin while excluding euchromatin. The presence of repressive histone mark – H3K9me3 – and protein HP1 works as a heterochromatin-specific cue. DIM2 tends to work on oligonucleosomes in order to maintain the repressive state of the chromatin,

preventing the exposure of the DNA strand. The multivalent interaction of DIM2 on higher-order nucleosomes also showed that DIM2 plays an essential role in further compaction of nucleosomes into heterochromatin. However, the presence of only essential amount of DIM2-HP1 complex is important since addition of relatively higher concentration of DIM2-HP1 complex to tetranucleosome may cause unwanted aggregation of the tetranucleosome due to multivalent character of DIM2. DIM2 recruitment and activity on oligonucleosome induce structural and epigenetic stability of highly compacted chromatin. Based on the proven possibility of different activities of nucleosome-interacting proteins on chromatin, there exist many opportunities to involve different nucleosome-interacting proteins that play important roles in condensing or loosening higher-order nucleosomes. Structural analysis of those interactions enables examination to enhance knowledge in storing or processing the basic fundamental units of genetic information in eukaryotic cells.

Reference

[1] Alvarado, W., Moller, J., Ferguson, A. L., & de Pablo, J. J. (2021). Tetranucleosome Interactions Drive Chromatin Folding. ACS Central Science, 7(6), 1019–1027. https://doi.org/10.1021/acscentsci.1c00085

[2] Basanta, B., Hirschi, M. M., Grotjahn, D. A., & Lander, G. C. (2022). A case for glycerol as an acceptable additive for single-particle cryoEM samples. Acta Crystallographica Section D Structural Biology, 78(1), 124–135. https://doi.org/10.1107/s2059798321012110

[3] Dombrowski, M., Engeholm, M., Dienemann, C., Dodonova, S., & Cramer, P. (2022). Histone H1 binding to nucleosome arrays depends on linker DNA length and trajectory. Nature Structural & Molecular Biology, 29(5), 493–501. https://doi.org/10.1038/s41594-022-00768-w

[4] Gallagher, J. R., Kim, A. J., Gulati, N. M., & Harris, A. K. (2019). Negative-Stain Transmission Electron Microscopy of Molecular Complexes for Image Analysis by 2D Class Averaging. Current Protocols in Microbiology, 54(1). https://doi.org/10.1002/cpmc.90

[5] GRIFFITH, J. D., & BONNER, J. F. (1973). Chromatin-like Aggregates of Uranyl Acetate. Nature New Biology, 244(133), 80–81. https://doi.org/10.1038/newbio244080a0

[6] Li, G., Margueron, R., Hu, G., Stokes, D., Wang, Y.-H., & Reinberg, D. (2010). Highly Compacted Chromatin Formed In Vitro Reflects the Dynamics of Transcription Activation In Vivo. Molecular Cell, 38(1), 41–53. https://doi.org/10.1016/j.molcel.2010.01.042

[7] Palovcak, E., Wang, F., Zheng, S. Q., Yu, Z., Li, S., Betegon, M., Bulkley, D., Agard, D. A., & Cheng, Y. (2018). A simple and robust procedure for preparing

graphene-oxide cryo-EM grids. Journal of structural biology, 204(1), 80–84. https://doi.org/10.1016/j.jsb.2018.07.007

[8] Richards, E. J., & Elgin, S. C. R. (2002). Epigenetic Codes for Heterochromatin Formation and Silencing. Cell, 108(4), 489–500. https://doi.org/10.1016/s0092-8674(02)00644-x

[9] Richmond, T. J., & Davey, C. A. (2003). The structure of DNA in the nucleosome core. Nature, 423(6936), 145–150. https://doi.org/10.1038/nature01595

[10] Shao, Z., Lu, J., Khudaverdyan, N., & Song, J. (2024). Multi-layered heterochromatin interaction as a switch for DIM2-mediated DNA methylation. Nature Communications, 15(1). https://doi.org/10.1038/s41467-024-51246-4

[11] Stark, H. (2010). GraFix: Stabilization of Fragile Macromolecular Complexes for Single Particle Cryo-EM. Methods in Enzymology, 109–126. https://doi.org/10.1016/s0076-6879(10)81005-5